Applied Laser Technology
Vol. 29, No.1,Jan (2022), pp.01–14

Molecular Dynamics Studies on the Denaturation of Polyalanine in the Presence of Guanidinium Chloride at Low Concentration

Boggavarapu Jyothy[1] , Johnmiya Shaik[2] , Ramanji Rao Bommagani[3] , Pillalamarri Anita Kumari[4] , Bavireddy Durgaprasad[5] , Assistant Professor1 , 2 , 3,4,5, Mail Id : jyothisrinivas2011@gmail.com,Mail Id : sonuminnu89@gmail.com, Mail id : bommaganiramanji@gmail.com, Mail Id : anitakumari.sbit@gmail.com,Mail Id : durgaprasad4me@gmail.com, Department of H & S, Swarna Bharati Institute of Science and Technology (SBIT), Pakabanda Street,Khammam TS, India-507002.

Abstract

In an explicit solvent, molecular dynamic simulation is a potent tool for keeping tabs on any and all atomic-level changes. Many chemical and metabolic parameters of large-scale biological systems may be calculated with this approach. In this study, polyalanine (PA) was simulated with all atoms at 273-395 K in the presence of 0.224, 0.448, 0.673, 0.897, and 1.122 M guanidinium chloride (GdmCl). An intermediate occurs between the helix and the coil, as evidenced by the analysis of surface area, radial distribution function, radius of gyration, heat capacity, hydrogen bonds, helix, coil, and beta contents. When present in small amounts, GdmCl slows the helix-to-coil transition, raises the transition temperature (Tm), and increases the number of solvent molecules in the hydration layer and interapeptide hydrogen bonds. Due to its similar effect on the beta form and the hydration layer and thermal stability of polypeptides, guanidine has a similar role at low concentrations.

Keywords: Polyalanine phase transition In terms of temperature, Thermal Conductivity: Medium

INTRODUCTION

Important biological consequences of the polyalanine (PA) peptide include the induction of several human diseases and neurodegenerative disorders [1]. Understanding the processes underlying these clinical illnesses and neurodegenerative disorders requires a thorough structural research of PA peptide to find their conformational features. There have been a number of theoretical and experimental investigations on the structural properties of PA peptide and its derivatives [2]. However, it is difficult to determine the conformational features of PA by experimental approaches due to its high insolubility in water, which causes these PAs to aggregate.

Research on fibril aggregate formation using peptide model systems has proved fruitful. Proteins with conformational disorders tend to aggregate because of the addition of extensive -sheet structure not present in the native state. Conformational diseases can be caused by variations in the sequence or structure of a protein. Amyloid fibrils are a common outward manifestation of conformational disorders.

The molecular mechanisms behind amyloid seed production and elongation are poorly understood, although progress in this area has the potential to yield new therapeutic and design strategies [3]. It has been challenging to gain atomic detail on peptide amyloid production from X-ray diffraction of amyloid fibrils because short peptide systems are much simpler than those of big proteins. Additionally, getting atomic information regarding seed production and spread is challenging using existing experimental methods. Given the high cost of traditional experimental approaches, computational tools such as molecular dynamics [5,6] and quantitative structure-activity relationships [6,7] can be useful in assisting with drug discovery.

Osmolytes have been shown to be an effective Alzheimer's disease therapy because of their ability to prevent protein aggregation. In light of these experimental findings, Liu and colleagues have used molecular dynamics simulations to examine the effects of trehalose (an osmolyte) on amyloid aggregation inhibition [5]. However, it is important to grasp the structural alterations in proteins because of the recognized link between structure and function. Denaturants, both thermal and chemical, can cause structural alterations.

[8,9] that may be investigated using several approaches [10–15].
The helix-to-coil phase transition in polypeptides is one of the most well-studied structural transitions. The helix-coil transition in polypeptides has been the subject of substantial experimental research [16]. Differential scanning calorimetry and circular dichroism methods [17] were used to measure the heat capacity and helicity of the polypeptide as a function of temperature, and infrared spectroscopy [18, 20] was used to examine the kinetics of the helix-coil transition of the 21-residue alanine polypeptide.
Protein structural alterations may also be induced by chemical species, it has been reported. The effects of solutes that may function as either a stabilizing agent or a denaturing agent have been the subject of a number of experiments. For instance, guanidine hydrochloride [24], urea [25], and surfactant [8] operate as denaturing agents, while ethylene glycol [21], certain salts [22], sugars, and polyols [23] are known to stabilize proteins in aqueous solutions.

Despite the fact that the precise mechanism of its denaturation capabilities remains unknown [26,27], guanidine cation is the most effective protein denaturant routinely utilized to research the protein stability and folding. Because numerous hydrogen bonds of amides in the hidden backbone are exposed upon unfolding, the binding of Gdm ions to polypeptides is thought to contribute significantly to protein denaturation. Denaturants, on the other hand, have been explained in terms of their influence on water's hydrogen-bond network, which increases the aqueous solubility of hydrophobic side chains revealed during unfolding.
The "stickiness" of Gdm+ ions is analogous to the "pushing" of weakly hydrated ions (chaotropes) onto weakly hydrated surfaces by substantially stronger water-water interactions, as described by Collins [28]. As was observed for Gdm and urea [29], denaturation occurs to some degree as a result of a favorable interaction with the polypeptide backbone revealed on unfolding. While peptide backbones interact positively with sugars and other polyols (osmolytes), they are selectively removed from the protein surface due to their unfavorable interactions with the peptide backbone [30]. These denaturants generate different perturbations at different locations, which may explain why certain residues prefer a helical secondary structure in the urea-denatured state and a more linear shape in the guanidine-denatured state [31].
The Fyn SH3 domain is greatly stabilized by guanidinium hydrochloride (GdmCl) at low doses [32]. The domain's unfolding rate is dramatically reduced due to the stabilizing impact, whereas the folding rate is changed just little. NaCl, on the other hand, stabilizes this domain by increasing the folding rate, therefore this action is counter to its impact. This suggests that GdmCl's stabilizing function is not primarily ionic. Many proteins have been hypothesized to bind particularly with guanidinium ion in addition to the arginine-containing ligands with which they are ordinarily associated. As a result, GdmCl should be utilized with caution as a denaturant in investigations of protein folding [32].
Because of its ionic nature, the effects of GdmCl on protein stability are highly nuanced. There are several ways in which ions might affect protein stability, including binding to the folded or unfolded state, "screening" columbic interactions, the Hofmeister effect, and altering the structure of the solvent [33,34]. Low doses of GdmCl have been shown to stabilize proteins [35-38], despite the chemical's reputation as a denaturant. It has been demonstrated that the ionic character of GdmCl is the primary factor in its stabilizing action in the majority of these situations [36,37]. However, GdmCl may affect protein stability in a more targeted fashion, as demonstrated by certain investigations [35].
In this research, we employ the MD method to investigate the - helix random coil phase transition in alanine polypeptides at varying temperatures in the presence of GdmCl. Helix, coil, and beta content variations are used to track the structural changes. Water and ions in the vicinity of a protein follow a radial distribution function. Heat capacity change at different temperatures and GdmCl concentrations is used to study protein stability and intermediate monitoring.

Simulation Details

Initial helix structure of polyalanine was created by Hyperchem 7.0 (Scheme 1). The N and C termini of polyalanine are capped, respectively, by neutral acetyl

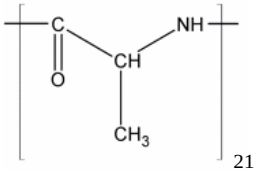

(a)

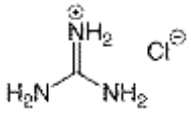

(b)

Scheme 1. Structure of a) polyalanine and b) guanidinechloride

amine groups, with 21 ALAS being the predicted sequence. The PRODRG2 server (http://davapc1.bioch.dundee.ac.uk/cgi bin/prodrg_ beta) [39] was used to construct the guanidinium chloride molecule's force field parameters and topology. The peptide was first contained within a periodic cube. The volume of the box used in the simulations was maintained constant at 70 nm3 by keeping the distance between the peptide and the box boundaries at around 1 nm. This allows us to discount the possibility of unintended consequences [40] from the periodic boundary conditions that have been imposed.

Finally, we randomized the addition of water molecules and Cl ions into the simulation box, ensuring that they would not overlap (Table 1).

First, the energy associated with the peptides was minimized, next the energy associated with the ions and water molecules (position constraint), and finally the energy associated with the whole system was minimized. The system was stabilized for 0.8 ns at 1 atm pressure and 273-390 K temperature after 400 energy reduction steps.

As a method for creating new shapes, high-temperature molecular dynamics is here considered. In order to access a large number of nearby local minima, high temperatures are used to provide the energy needed to overcome energetic barriers. High temperature molecular dynamics and direct conformational search were compared, and the findings indicated little overlap in conformational space [41,42]. At the lower temperature, the direct technique covered more of the conformational space than molecular dynamics, but at 1500 K, the two methods covered the same amount of space. High-temperature molecular dynamics was shown to be useful in assisting conformational searches. Such high temperatures are of curiosity for structural space exploration, but they have little physical significance. When applied to peptide segments on the order of a dozen residues or more—perhaps more for a cyclic system—high-temperature molecular dynamics provides an acceptable conformational search tool. MD modeling often takes this range into account.

For all of our MD simulations, we used the GROMACS 3.3 program [43] in conjunction with the GROMOS96 force field [44]. SPC stands for the "simple point charge" model.

Table 1. Number of Guanidine and Chloride Ions and Number of Water Molecules in the Molecular Dynamics Box

Guanidine concentration (M)	Number of guanidine ions	Number of water molecules	Number of chloride ions
0	0	2296	0
0.224	10	2279	10
0.448	20	2265	20
0.672	30	2252	30
0.896	40	2241	40
1.122	50	2228	50

ISSN: 1000-372X ALT

meaning "water" in [45] context. The equations of motion were integrated using the Verlet technique at a time step size of 2 fs [46]. Each run took a total of 20 ns to simulate. The distribution function (RDF) or pair correlation function gAB(r) between particles of type A and B is defined as follows, and it was used to account for the long-range electrostatic interactions:

The Ewald technique of particle meshes [47]. The list of atoms that don't form a bond

The nstlist was refreshed every (2) 10 steps, and the cutoff was set at 0.9 nm. All bond lengths were constrained using the LINCS technique [48].

The Nose-Hoover thermostat [49, 50] and the Parrinello-Rahman barostate [51] with coupling constants of 0.1 and 0.5, respectively, were used to regulate the temperatures (273-390 K) and the pressure (1 atm). Every 50 ps, the atomic coordinates were recorded during all simulations. The MD simulations were executed on a Rocks network clustered with 40 CPUs. Three separate iterations of each computation yielded the same findings (Fig. S1).

where B>local is the average density of type B particles in all spheres of radius rmax around particles A, and B>(r) is the density of type B particles at distance r around particles A. The maximum radius, or rmax, is typically taken to be equal to half the box length. The radius of gyration is quantified by the "g_gyrate" variable. The "compactness" of the building may be described by this number. This is computed as follows and provides a measure of the atom(s)' mass in relation to the molecule's center of mass.

Analyses

Several supplementary programs included in the GROMACS 3.3 package were used to examine the simulated trajectories. All sorts of helix attributes may be calculated using the "g_helix" key. The percentage of helices, coils, and betas was also determined with the use of VADAR [52]. The "g_rms" measures the average amount by which the structure has changed from its initial state during the simulation. The relative mean square deviation (RMSD) between a set of atoms in a molecule and a reference structure can be computed as follows:

Where mi is the mass of atom i and ri is atom i's relative location to the molecule's center of mass. The "g_sas" function determines the solvent-molecule-accessible surface of the peptide. Using the fluctuation theorem [20], we have determined the heat capacity of the system while considering the polypeptide in the NPT ensemble:

Both the backbone and the whole protein may be used to calculate the RMSD. Hydrogen bond interactions between hydrogen donors and acceptors are calculated using the "g_hbond" function. If the distance between the donor and the acceptor is less than 0.35 nm and the angle between the donor and the hydrogen acceptor is less than 30 degrees, then the hydrogen bonds are regarded to be unbroken. Radial distribution functions may be computed in several ways using the "g_rdf" function. The first strategy revolves around the particle(s) itself, whereas the second strategy revolves around the mass center of the particles. The study took into account the molecular centers of mass. In this equation, H is the enthalpy of the polypeptide as a function of time, Hi is the enthalpy of the ith state, and k is the Boltzmann constant. Equation (5) is a summation across all possible system states. During the simulation, GROMACS was used to directly get the average total configurational energies E + PV, as shown in the equation H = E + PV.

RESULTS AND DISCUSSION

Time Evolution

During the 20 ns computation, the effect of varying guanidinium chloride concentrations and temperatures on polyalanine structure was studied. Molecular diagram depicting the location of guanidine and chloride ions in close proximity to polyalanine (Fig. 1).

Fig. 1 demonstrates that guanidine chloride denatures polypeptide, leading to unfolded polypeptide, a drop in helix percent, and a rise in coil size at the beginning of the simulation. Midway through, the beta structure heightens, and then the coil percentage rises. All helix structure transforms into a coil at elevated temperatures. This point is reinforced by the explanation

of Fig. 2.

Denaturants can change the structure of polypeptides in two ways: 1) by direct contact, which is quite particular, and 2) through indirect, which is very general, and affects the solvent distribution. The majority of the Fig. 1 screenshots depict generic interactions, which are addressed elsewhere in the text. Reagents that are salted in, like urea and guanidine, pull water away from neighboring proteins, increasing the unfolding of the polypeptide, whereas reagents that are salted out, like sodium chloride, push water around the polypeptide, increasing its folding.

Water molecules are omitted to simplify the illustration. Hydrophobic, hydrophilic, and total solvent accessible surface (SAS), intramolecular hydrogen bonds (HB-p-p), intermolecular hydrogen bonds (HB-p-sol), radius of gyration (Rg), root mean square deviation from carbon alpha (RMSD), and percents of helix, beta, and coil are shown in Figure 2 as they change over time.

The hydrophobic SAS variation is steeply dropping until 8500 ps, plateauing between 8500 and 16500 ps (dotted rectangle), and then gradually increasing till 20000 ps. The hydrophilic surface variation peaks at around 3000 ps and gradually diminishes thereafter. The overall surface is very much like a hydrophobic one. It appears that hydrophilic groups become increasingly solvent-exposed, while hydrophobic groups are often found deeper within the polypeptide.

The HB-p-sol curve exhibits an upward tendency up to 4500 ps, followed by a downward trend until the end time. Rg follows the same general trend as the total surface and HB-p-p, but in the opposite direction of RMSD. This means that early on, protein-protein interactions are weaker while those with the solvent are stronger.

Importantly, the next parts will focus on the occurrence of a peak between 10000 and 15000 ps.

Temperature Effect

Figure 2 shows the impact of temperature on the mean of the variables (over the past 2 ns) mentioned in the first column. Increasing temperatures are known to cause polypeptides to unfold, and hence increase denaturation. It causes the structure to transform from a helix to a random coil. Boosting the temperature has the effect of expanding the polypeptide's accessible surface area and shrinking its hydrophobic and electrostatic interactions. Hydrophilic surface area, RMSD, coil%, and beta% rise as temperature lowers, whereas hydrophobic surface area, total surface area, radius of gyration, and intramolecular hydrogen bond decrease. The initial phase appears to involve a modification of the helix structure and the observance of partial unfolding. Some of the amino acids that were previously folded into the protein's structure now interact with each other to produce a new helix or beta structure. Therefore, it is possible that the creation of beta and helix structures, which reduces surface area, impedes correct unfolding. An unfolding event transforms the helix conformation into the random coil or beta, which has a smaller radius of gyration.

Effect of Guanidine Chloride

Figure 2's last column depicts the influence of low concentrations of guanidine on the mentioned physical characteristics. The overall SAS and the hydrophobic SAS both tend upwards. In contrast to hydrophobic surfaces, intermolecular hydrogen bonds (HB-pro-pro), RMSD, and coil percentages, hydrophilic surfaces, polypeptide solvent hydrogen bonds (HB-pro-sol), Rg, and helix percentages all move in the other direction.

Molecular Interactions Monitoring

The snapshot of the process was captured at several time frames to shed light on these events at the molecular level. As can be seen in Figures 3a–d, the polypeptide first adopts a mostly helical conformation.

ISSN: 1000-372X ALT

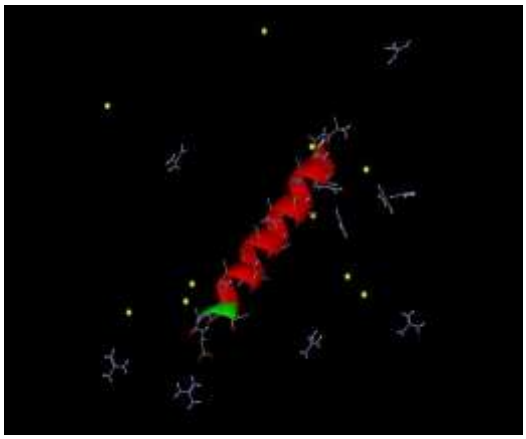

0 ps

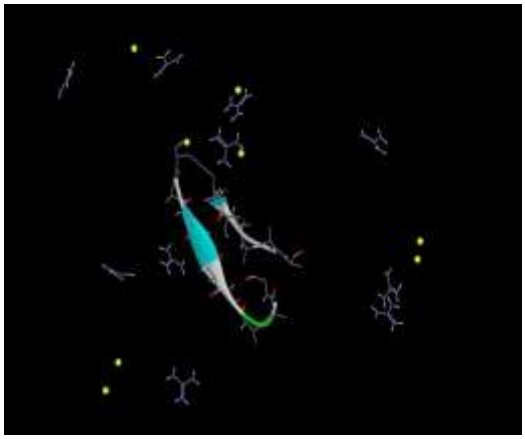

8000 ps

16000 ps

ISSN: 1000-372X ALT

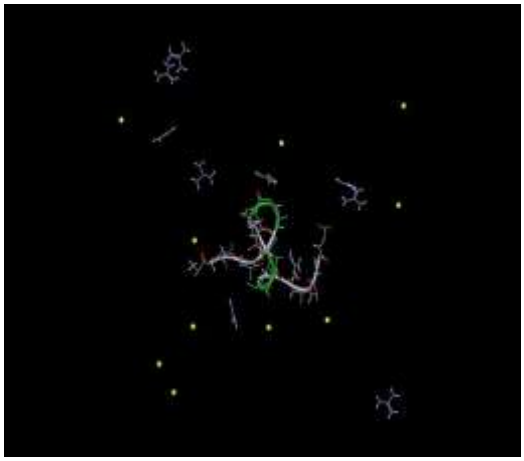

4000 p

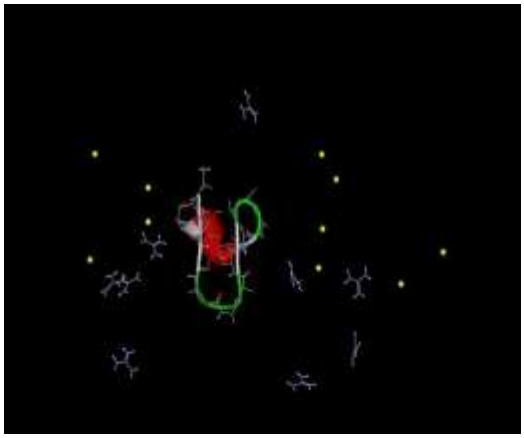

12000 ps

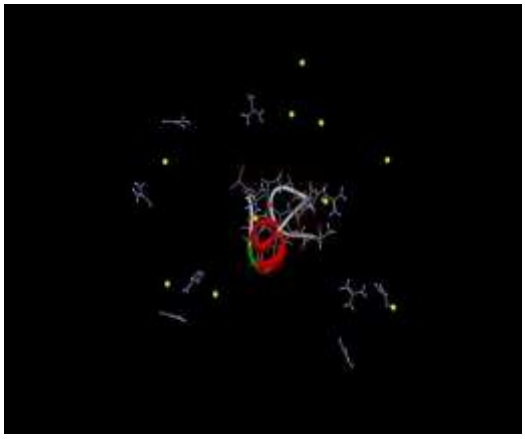

20000 ps

Fig. 1. Molecular snapshot of 10 molecular ions of guanidine chloride around polyalanine at 345 K. Red ribbons, blue, green, and white bands represent helical structure, beta sheet, turn and coil structure, respectively. Chloride ions were shown by yellow dot.

ISSN: 1000-372X ALT

Applied Laser Technology
Vol. 29, No.1,Jan (2022), pp.01–14

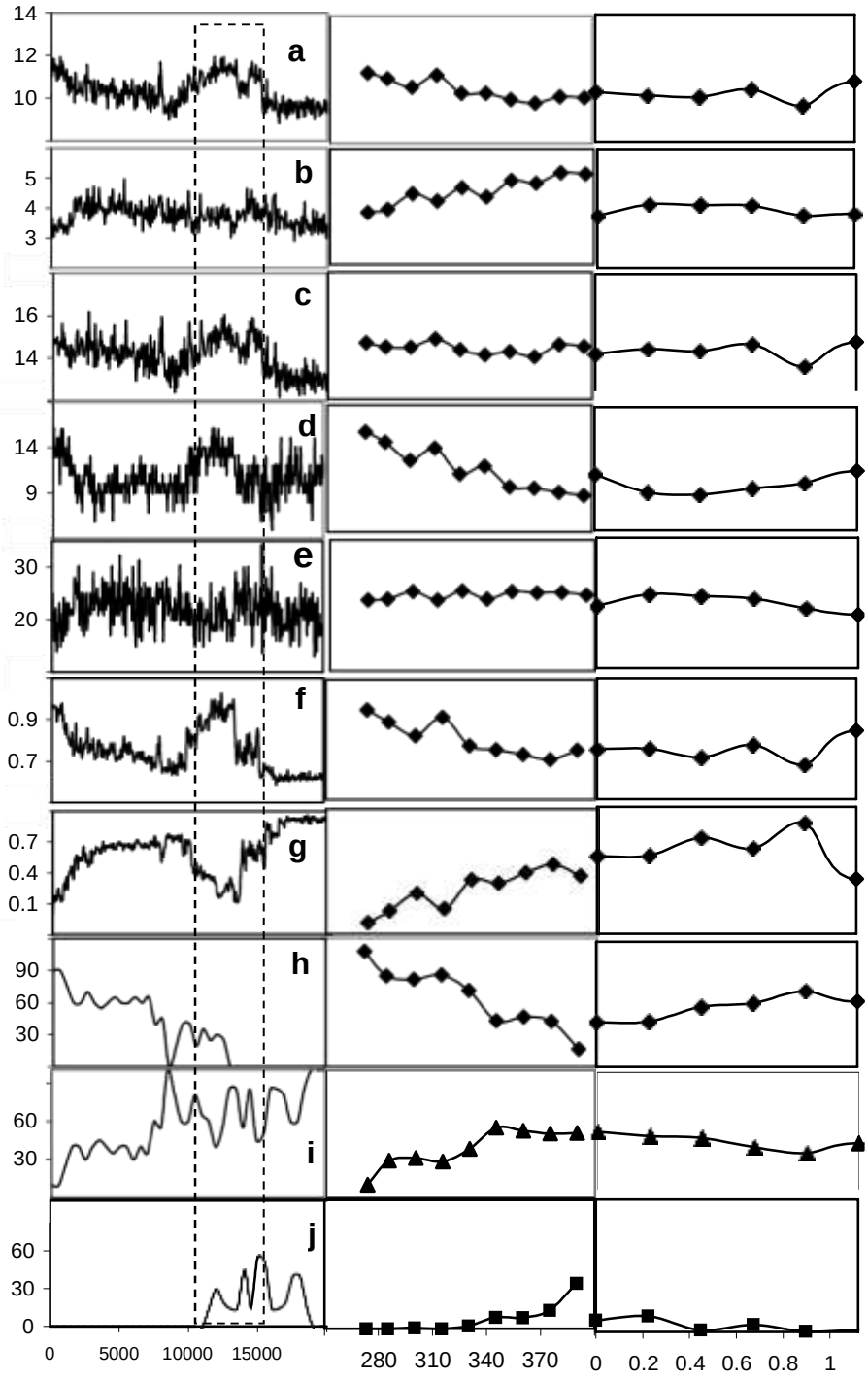

The split is around 85% to 15%. At 5500 ps, poly alanine undergoes a flawless structural conversion to the coil and the beta

ISSN: 1000-372X ALT

state. At 6000 ps, the beta parallel is clearly visible. After the systems are changed to each other, just the beta and coil remain. These exchanges vary across the time period under study; as the beta rises, the coil falls, and vice versa.

At 14500 and 17000 ps, the anti parallel beta structure appears; at 19000 ps, the polypeptide is transformed to the coil and remains in this state until the end.

Because the system is more complex than a simple two-state model, it requires transition stages. The three-state model is the focus of this paper. Here, we see helix transformed into beta and coil. In such setting, beta conformation became apparent. Since beta production does not occur at all temperatures, kinetic study could not be performed under all circumstances. Therefore, only the first-order activation energy for converting helix to product can be estimated.

k h product

Consequently, the partially unfolded intermediate state may be associated with beta formation and/or helix reformation. In particular, the unfolding of a polypeptide exposes solvent-accessible hydrophobic patches, which increases the likelihood that hydrophobic groups at various places may interact. As a result, the polypeptide takes on a more ordered and stable beta form. Increases in intra-peptide hydrogen bonds, secondary structure, and reductions in surface area and RMSD are all effects of beta production. Figures 3b-d show the helix, coil, and beta content calculated by the VADAR server [52]. We

By plugging these percentages of helix time into the previous equation, we can get the rate constant (k). In order to determine the values of k, this procedure must be repeated under other conditions, most notably at greater temperatures. It should be borne in mind that the fitting error is less at higher temperatures than at lower ones. The activation energy (Ea) is calculated from the slope of the lnk vs. 1/T (Fig. 3f) plot using the Arehnius equation (Eq.

For this study, we used a sequential kinetic mechanism (k = Ae = Ea / RT) to look at the transition from helix to beta and coil. Therefore, the equations of motion for the transition from the helix to the coil must include

The Ea is then graphed vs guanidine concentration. when can be seen in Fig. 3g, when the quantity of guanidine rises, so does Ea. Low concentrations of guanidine appear to maintain the helix shape and slow the pace at which it converts to a coil.

It has been proved that guanidine denatures the macromolecule by two ways. One is related to direct effect on the macromolecule which is due to direct hydrogen bond,

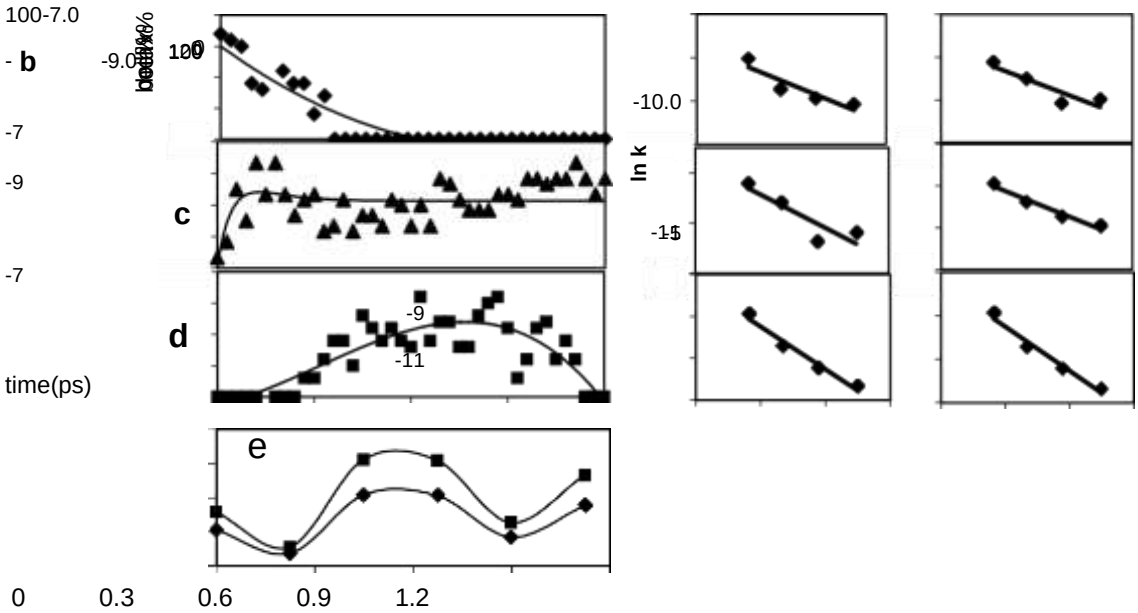

Fig. 3. (VADAR's (b) helix, (c) coil, and (d) beta percents (scatter data points) during a 20 ns molecular dynamics simulation, as well as the fitted (solid) line obtained from the data using equation (6). (e) The shift in the first (k1) and second (k2) rate constants in the helix-to-coil conversion equation (6) (f) the dependence of lnk on the inverse of temperature for varying concentrations of guanidine, and (g) the dependence of the activation energy calculated using Eq. (8) on the concentration of guanidinium chloride.

whereas stabilizing substances are kept away from the protein and push water to congregate close by. Therefore, the local and distant movements of all denaturant, solvent, and ion species are tracked. This was done by calculating the RDF of the water and ligand around the peptide backbone atoms and then using that information to describe the local distribution of water and guanidine molecules in MD trajectories (Eq. (2)).

ISSN: 1000-372X ALT

Distinct solvent and guanidine RDF patterns surrounding protein and guanidine ions are seen in Figure 4.

The relative dissociation factor (RDF) of polyalanine in water at varying concentrations of GdmCl is shown in Figure 4a. The RDF is shown at 0.3 nm in the inset of the picture and in its extended forms (parts b and c). It rises to 0.672 M guanidine, where it peaks, before falling at 0.896 M and 1.122 M. This suggests that GdmCl increases the amount of water around the protein at low concentrations and lowers it at high concentrations. On the other hand, the RDF's tendency at greater distance is the opposite of its trend at lesser distance. Therefore, guanidine acts like an osmolyte (such as trehalose) at low concentrations (less than 0.896 M) [5], and like urea and other denaturants at greater concentrations.

The RDF for the Gdm ion surrounding the protein is shown in Figure 4d. As ion concentration increases, both close to and distant from the protein, it decreases. Bar lines in Figs. 4d–4h are not labeled because of space constraints. From left to right, the bar lines in Figs. 4d–4h represent guanidinium chloride concentrations of 0.224, 0.448, 0.672, 0.896, and 1.122 M. Using the notion of preferred hydration and exclusion, we were able to better understand this phenomenon. The stabilizing impact of protective osmolytes on proteins is often attributed to this. According to the proposed mechanism, thermodynamic stability is achieved by an increase in the number of water molecules in the hydration shell surrounding the proteins as a result of the exclusion of osmolyte molecules from the protein/solvent contact. Here, we may examine the preferred hydration of peptides in guanidine solutions by looking at the distributions of water and guanidine. Different amounts of guanidine in RDF protein are depicted in Figure 4d. With increasing guanidine concentration, the peptides become preferentially hydrated within a distance of roughly 0.3 nm from the nearest backbone atoms of polyalanine. At greater distances, there is a considerable water gradient in contrast to the preferential hydration on the peptides.

shortage caused by an abundance of guanidine molecules. Therefore, it may be deduced that low-concentration guanidine solutions have a narrow hydration shell on the surface of the peptides. What this means is that when the quantity of guanidine rises, the water molecules atop the peptides actually get more concentrated. The experimental finding that osmolytes in water are completely excluded from the initial hydration shell of proteins [22] is consistent with these findings.

Long-range protein choloride interactions are reduced but short-range interactions are enhanced as GmCl concentration is increased (Figure 4e). What this means is that the chloride ion gravitates toward the protein molecule. Figure 4f displays the radius distribution function (RDF) of water around ligand (Gdm). Its concentration is lowered throughout the board. Both Figure 4d and 4f demonstrate that an increase in guanidine concentration causes the guanidinium ion to move further from the protein and become more solvated. Figure 4g displays the reverse distance function (RDF) for guanidine-guanidine (Gdm-Gdm), which decreases in the close and increases at the far distance. Because guanidine tends to collect distant from polypeptides in the same way as osmolytes do, the concentration of guanidinium ions in RDFs drops in the vicinity of protein. Chloride ion (RDF) distribution surrounding Gdm is shown in Figure 4h. The reduction in this metric indicates that the chloride ion has relocated to a position close to the peptide.

However, many proteins exhibit a dramatic rise in Cp during unfolding, suggesting that the unfolding entropy and enthalpy are very temperature dependent. The exposure (solvation) of polar and nonpolar groups causes variations in the hydration heat capacity, which in turn causes changes in Cp related with protein unfolding. The average length and angle of the water-water hydrogen bonds in the initial hydration shell are both reduced when nonpolar solutes are present, but they increase when polar or ionic solutes are present. This is because there is a shift in the ratio of two types of hydrogen bonds, those that are shorter and more linear and those that are longer and more curved [54].

Heat capacity and percentages of helix, coil, and beta, as well as temperature dependence, for polyalanine in the absence and presence of 0.876 M and 1.122 M guanidine ions are displayed in Figure 5. Helix percentage goes down and beta and coil percentage go up when temperature goes up in guanidine deficiency.

ISSN: 1000-372X ALT

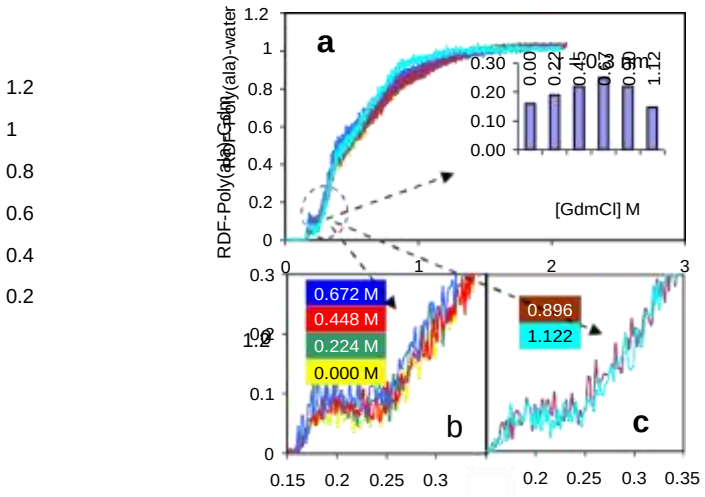
a
b
c
[GdmCl] M
0.672 M
0.448 M
0.224 M
0.000 M
0.896
1.122
RDF-Poly(ala)-Gdm
RDF-Poly(ala)-water

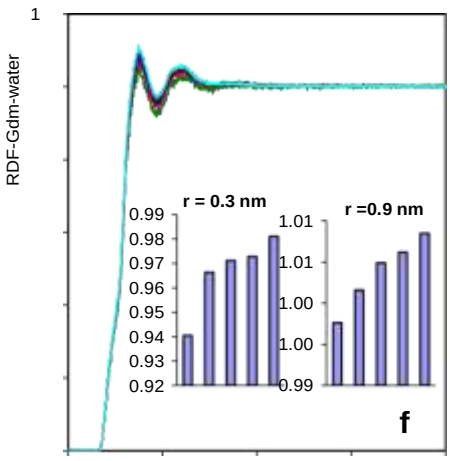
f
r = 0.3 nm
r =0.9 nm
RDF-Gdm-water

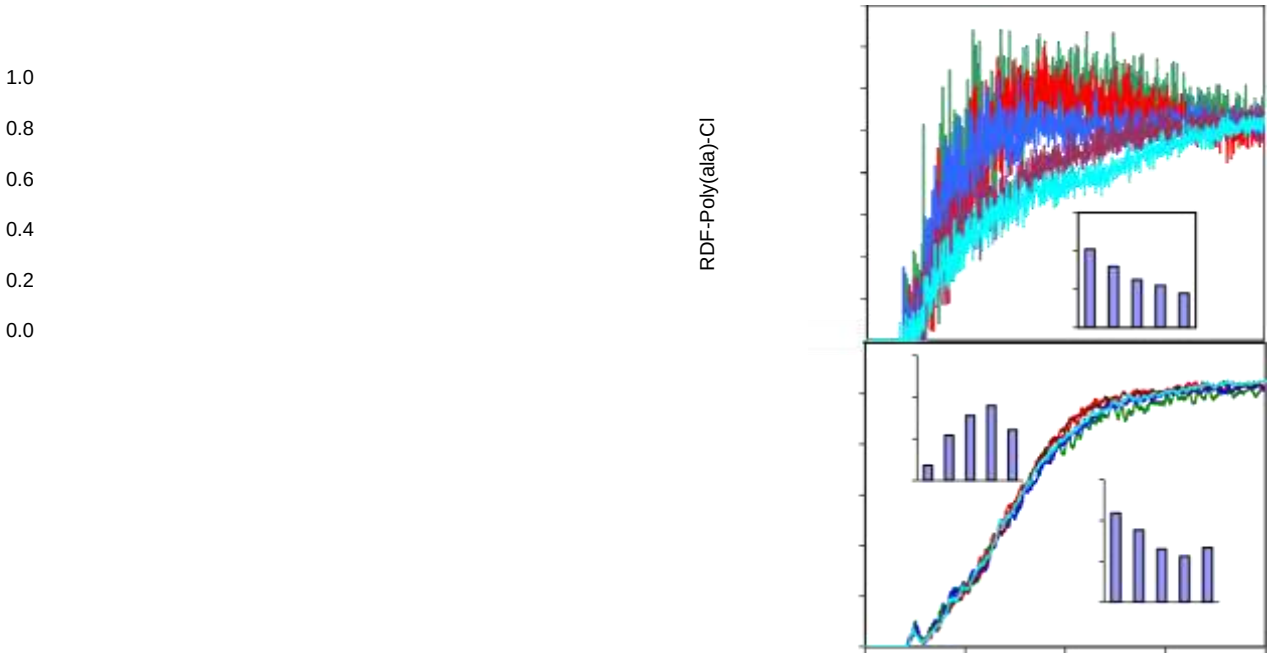
RDF-Poly(ala)-Cl

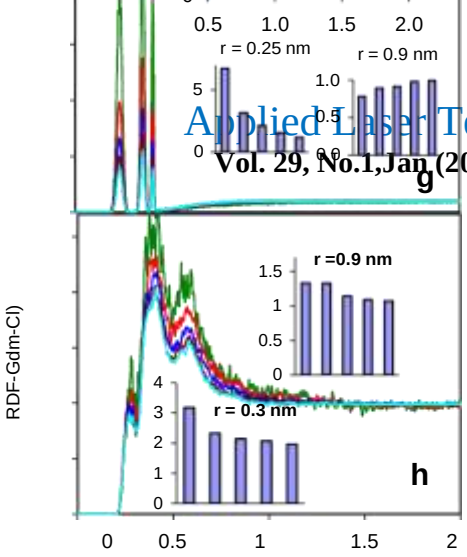

0
2.5
2.0
1.5
1.0
0.5
0.0

Fig. 4. RDF plots for water around polyalanine's center of mass in the absence (yellow) and presence of guanidinum chloride at concentrations of 0.224 M (green), 0.448 M (red), 0.672 M (blue), 0.896 M (brown), and 1.122 M (turquoise): (b) expanded plot for low concentration; (c) expanded plot for high concentration. Polyalanine surrounded by guanidinium (d) and chloride ions (e) of the RDF. The guanidinium ion is surrounded by an RDF consisting of water molecules (f), guanidinium (g), and chloride ions (h). Similar to (a), the horizontal axis of the bar line graphs depicts the [GdmCl] in molar form. The concentrations of guanidinium chloride shown in the inset of Figure 3 (excluding Part a) are 0.224 M, 0.448 M, 0.672 M, 0.896 M, and 1.122 M, respectively.

Helix and coil variations are exactly antiparallel to one another in the absence of a beta dosage. However, the previous order is not established when the beta appears at higher temperatures since the total of the helix, the coil, and the beta must be 100%. Furthermore, both the helix and coil% curves have two troughs or peaks. The first peak is associated with the transition from a helix to a partially unfolded (beta and/or reformed) structure, while the second peak is associated with the transition from a beta and/or reformed helix to a fully coil configuration. Figures 5b and 5c depict the percentages of helix, coil, and beta in 0.673 and 1.122 M guanidine ion, respectively. Peaks shift to the right when concentration is increased, as shown in comparison to section (a).

Figures 5d-f depict the Cp values vs temperature for three different guanidine concentrations. In terms of curve form, we have

somewhat analogous to thermograms generated by differential scanning calorimetry. DSC is typically employed in the study of macromolecule thermal stability [10]. Corresponding percentages of helices, coils, and betas are also shown. Two peaks, one at 300 K and one at 360 K, may be seen in Figure 4a. Polypeptide has two Tms. The first Tm is involved in the transition from the helix to the beta form, while the second Tm is involved in the transition from the beta form to the unfolded coil. The melting point (Tm) of polypeptides has been found to be in the ambient temperature range [55]. Denaturation is accompanied by an increase in Cp and a decrease in helix (Figure 5, dashed rectangle), indicating that the Cp trend is the exact opposite of the helix trend and the same for the coil and the beta form.

The curves in Figures 5b and 5c are equivalent to those in the

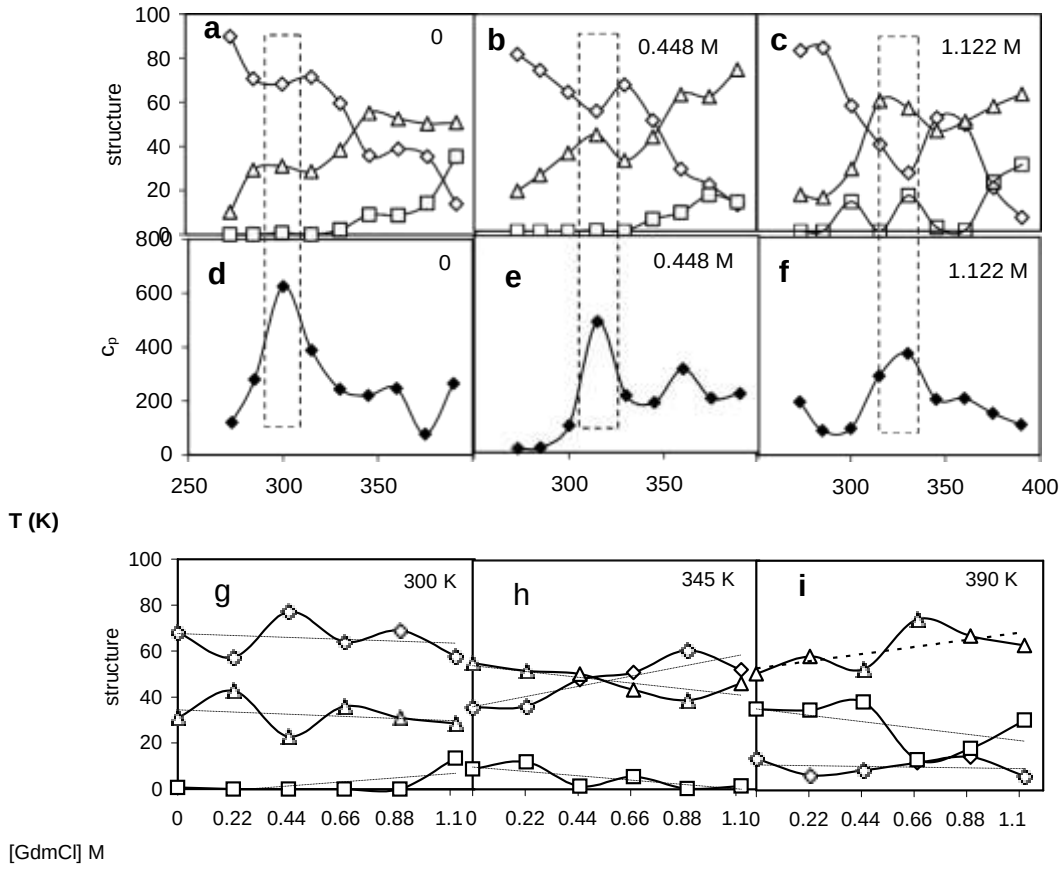

Fig. 5. Helix (◇), coil (△), beta (☐) contents in percent and heat capacity (✦) *vs*. temperature at three concentrations of GdmCl (a-f). Helix, coil, beta percents *vs*. guanidinium chloride concentration at three temperatures (g-i).

both 0.673 and 1.122 M GdmCl are present. Cp fluctuation trend is negatively correlated with helix and positively correlated with coil and beta. Without GdmCl, the initial Tm of polypeptide is 300 K, but with 0.673 M and 1.122 M GdmCl, the Tm increases to 315 K and 330 K, respectively. Since the ligand appears to boost Tm and protein stability, this would indicate that it does so. This theory is supported by a scatterplot showing the change in helix, coil, and beta at 300, 345, and 390 K for varying concentrations of guanidine.
The coiling trend is the opposite of the helixing one, and the beta structure is only observed between 0.896 and 1.122 M guanidine. At 345 K, the sum of the helix and the coil is smaller than it was at 300 K, and it decreases with guanidine. Total beta, on the other hand, is greater than 300K and trending downwards. The overall quantity of coil and beta is greatest around 390 K, whereas the amount of helix is least at lower temperatures.

CONCLUSIONS

The most widely used denaturant that causes protein unfolding at high concentrations is guanidium chloride. Nonetheless, there are a lot of indications that, like osmolytes, it stabilizes the macromolecues at low concentration. The activation energy and the transition temperature (Tm) between the helix and the coil phases are both raised. On the other hand, it expands the polypeptide's hydration shell as measured by the radial distribution function. In addition, it is driven off the polypeptide's surface, where it can no longer inhibit beta production or interamolecular interactions. As a result, it can be a tool in the fight against clustering and the illnesses it breeds. This kind of behavior has been seen in the osmolyte situation as well.

ACKNOWLEDGEMENTS

Damghan University's research council and IT center are thanked for their generous funding.

REFERENCES

[1] This was published in Mol. Model. 13 (2007) 1141 by B. Leitge, A. Kerényi, F. Bogár, G. Paragi, B. Penke, and G. Rákhely.
[2] J. Phys. Chem. B. 111, No. 2 (December 2007): 605 (S. Yang, M. Cho).

Specifically, [3] R.W. Carrell and D.A. Lomas in Lancet 350 (1997) 134.
Bioorg. Med.Chem. Lett. 19 (2009) 654 [4] L.J. Simons, B.W. Caprathe, M. Callahan, J.M. Graham, T. Kimura, Y. Lai, H. Levine, A.W. Lipinski, A.T. Sakkab, Y. Tasaki, L.C. Walker, T. Yasunaga, Y. Ye,. N. Zhuang, C.
J. Phys. Chem. B 113 (2009) 11320 [5] F.-F. Liu, L. Ji, X.-Y. Dong, Y. Sun.
To cite this article: [6] D. Ajloo, A.A. Saboury, N. Haghi-Asli, G. Ataei- Jafarai, A.A. Moosavi-Movahedi,, M. Ahmadi, K. Mahnam, S. Namaki, J. Enzym. Inhib. Med. Chem. 22 (2007) 395.
[7] A.A. Moosavi-Movahedi, S. Safarian, G.H. Hakimelahi, G. Ataei, D. Ajloo, S. Paojehpour, S. Riahi, M.F. Mousavi, S. Mardanyan, N. Soltani, A. Khalafi-Nezhad, H. Sharghi, H. Moghadamnia, A.
Colloids, Surfaces B, Biointerfaces 26 (2002) 185, D. Ajloo, A.A. Moosavi-Movahedi, G.H. Hakimelahi, A.A. Saboury, H. Gharibi.
Bull. Korean Chem. Soc. 23 (2002) 1073, A.K. Bordbar, A. Nasehzadeh, D. Ajloo, K. Omidiyan, H. Naghibi, M. Mehrabi, H. Khajehpour, M. Rezaei- Tavirani, A.A. Moosavi-Movahedi.
Thermochim. Acta 408 (2003) 9 by M. Rezaei-Tavirani, A.A. Moosavi-Movahedi, S.Z. Moosavi-Nejad, J. Chamani, and D. Ajloo.
J. Chem. Phys. 131 (2009) 214503; P. Dasmeh, D. J. Searles, D. Ajloo, Denis J. Evans, and Stephen R. Williams.
X. Wu and G. Narsimhan, "Molecular Simulation" 35, no. 974 (2009).
In Molecular Simulation 33 (2007) 1105, K. Bisetty, H.G. Kruger, and J. J. Perez were cited as the authors.
C. Niedermeier and K. Schulten, "Molecular Simulation 8 (1992) 361," cited in [14].
Int. J. Biol. Macromol. 43 (2008) 151, D. Ajloo, E. Taghizadeh, A.A. Saboury, E. Bazyari, K. Mahnam.
Phys. Rev. E 51912 (2007) 1. I.A. Solov'yov, A.V. Yakubovich, A.V. Solov'yov, and W. Greiner.
[17] J. Amer. Chem. Soc. 123 (2001) 2388; I.K. Lednev, A.S. Karnoup, M.C. Sparrow, and S.A. Asher.
Biochemistry 35 (1996) 691 S. Williams, R.G. Thimothy P. Causgrove, K.S. Fang, R.H. Callender, W.H. Woodruff, R.B. Dyer.
[19] S. Yang and M. Cho, Journal of Physical Chemistry B 111, no.
Specifically, this is a reference to [20] A.V. Yakubovich, I.A. Solov'yov, A.V. Solov'yova, W. Greiner Eur. Phys. J. D 51 (2009) 25.
J. Mol. Struc.-Theochem. 808 (2007) 93, by O.V. de Oliveira, A.F. de Moura, and L.C.G. Freitas.
Based on the research of T. Arakawa, R. Bhat, and S.N.
Based on the work of Y. Kita, T. Arakawa, T.Y. Lin, and S.N. Timasheff (Biochemistry 33, 1994), p. 15178), [23].
Biochemistry, vol. 43, no. 9589 (2004) [24] J. Fitter, S. Haber-Pohlmeier.

Proc. Natl. Acad. Sci. USA 105 (2008) 16928, L. Huaa, R. Zhoua, D. Thirumalaic, B. J. Bernea.
Proc. Natl. Acad. Sci. 100 (2003) 4557; T.P.E. Mason, G.W. Neilson, C.E. Dempsey, A.C. Barnes, J.M. Cruickshank.
Biophysical Journal 71 (1995) 2056 [27] ; R.L. Baldwin.
To cite this section: [28] K.D. Collins, Proc. Natl. Acad. Sci. USA 92 (1995) 5553.
Proteins 31 (1998) 107, Q. Zou, S.M. Habermann-Rottingaus, and K.P. Murphy.
Biochemistry 36 (1997) 9101 [30] A. Wang, D.W. Bolen.
[31] S. J. Chugh and R.V. Hosour, Arch. Biochem. Biophys. 481.109 (2009) 169.
Protein Science 162 (2006) 152, A. Zarrine-Afsar, A. Ittermaier, L. Kay, and A. Davidson.
Biophys. Chem. 96 (2002) 91, as cited by J.A. Schellman [33].
Collins, K.D. [34] Methods 34 (2004) 300.
Biochemistry 32 (1993) 7994 [35] - L.M. Mayr and F.X. Schmid.
Protein Science 3 (1994) 1984 [36] O.D. Monera, C.M. Kay, R.S. Hodges.
Protein Science 7 (1998) 689, by G.I. Makhatadze, M.M. Lopez, J.M. Richardson, and S.T. Thomas.
Acta Crystallogr. D 60 (2004) 1355; A.W. Schuttelkopf & D.M. van Aalten, Biochemistry 41 (2002) 13386; A.K. Bhuyan, Biochemistry 41 (2002) 13386.

J. Phys. Chem. B 104 (2000) 3668, W. Weber, P.H. Hunenberger, and J.A. McCammon.
[40] Reference: R.E. Bruccoleri & M. Karplus, Biopolymers 29 (1990) 1847.
J.L. Rosas-Trigueros, J. Correa-Basurto, C.G. Bentez- Cardoza, and A. Protein Sci. 12 (2011) 2035 [41].

Based on the work of D. Van Der Spoel, E. Lindahl, B. Hess, G. Groenhof, A.E. Mark, and H.J. Berendsen, which may be found in Comput.
Biomolecular Simulation: The GROMOS96 Manual and User Guide (Zürich, Switzerland; Groningen, Holland); I.G. Tironi; W.F. Van Gunsteren; S.R. Billeter; A.A. Eising; P.H. Hunenberger; P. Kruger; A.E. Mark; W.R.P. Scott; I.G. Tironi; 1996).
In: B. Pullman (Ed.), Interaction Models for Water in Relation to Protein Hydration [44], by H.J.C. Berendsen, J.P.M. Postma, W.F. van Gunsteren, and J. Hermans. Reidel: Dordecht, Holland, 1981, pp. 331-342 in Intermolecular Forces.
Computer Physics Review 159 (1967) 98 [45]. L. Verlet.
J. Chem. Phys. 98 (1993) 10089 [46] - T. Darden, D. York, L. Pedersen.
Comput. Chem. 18 (1997) 1463 [47] B. Hess, H. Bekker, H.J.C. Berendsen, J.G.E.M. Fraaije.
Nosé, S., Mol. Phys. 52 (1984), p. 255.
Phys. Rev. A 31 (1985) 1695 [50] - W.G. Hoover.
L. Willard, A. Ranjan, H. Zhang, H. Monzavi, R.F. Boyko, B.D. Sykes, D.S. Wishart, Nucleic Acids Research. 31 (2003) 3316; M. Parrinello, A. Rahman, Phys. Rev. Lett. 45 (1980) 1196; R.F.
Specifically, [53] J.I. Steinfeld, J.S. Francisco, and W.L. Hase. Printice-Hall International Edition, New Jersey, 1983, Chemical Kinetics and Dynamics.
280 (2005) 19343; A.V. Persikov, J.A.M. Ramshaw, and B. Brodsky, J. Biol.
[55] K.A. Sharp and B. Madan, Journal of Physical Chemistry B 101 (1997) 4343.